Laser interaction based on resonance saturation (LIBORS): an alternative to inverse bremsstrahlung for coupling laser energy into a plasma

R. M. Measures, N. Drewell, and P. Cardinal

Resonance saturation represents an efficient and rapid method of coupling laser energy into a gaseous medium. In the case of a plasma superelastic collision quenching of the laser maintained resonance state population effectively converts the laser beam energy into translational energy of the free electrons. Subsequently, ionization of the laser pumped species rapidly ensues as a result of both the elevated electron temperature and the effective reduction of the ionization energy for those atoms maintained in the resonance state by the laser radiation. This method of coupling laser energy into a plasma has several advantages over inverse bremsstrahlung and could therefore be applicable to several areas of current interest including plasma channel formation for transportation of electron and ion beams, x-ray laser development, laser fusion, negative ion beam production, and the conversion of laser energy to electricity.

Introduction

In many diverse applications lasers are used to heat and ionize a medium. In the plasma field the most well-known examples are: laser fusion; x-ray laser development; and laser heating of magnetically confined plasmas. There is also some interest in the possibility of converting laser energy into electrical energy for space probes via a thermoelectric process.[1] In almost all cases inverse bremsstrahlung plays the important role of converting laser energy into plasma energy.

The purpose of this paper is to show that laser saturation of an atomic resonance transition of some major constituent of a gaseous medium represents an attractive alternative mechanism for coupling laser energy into the medium, whether it be a plasma or cold and un-ionized. Measures[2] was the first to suggest that this approach could be used to enhance substantially the ionization of a plasma. According to Measures,[2] laser resonance saturation leads to both a heating of the electrons via superelastic collision quenching of the overpopulated resonance level and an effective reduction of the ionization energy of such laser excited atoms by the photon energy. These two effects lead to a very rapid and almost complete ionization of the medium, once the electron density exceeds some threshold value. Just prior to ionization burnout, however, there is a very rapid rate of laser energy deposition into the plasma.

If the medium is cold initially, there are several mechanisms for generating the seed electrons. If the laser irradiance is high (several orders of magnitude greater than needed to saturate the transition), multiphoton ionization from the resonance level is likely to predominate in creating these initial free electrons.[3,4] On the other hand, for more modest values of the laser irradiance, associative ionization can (for many atoms) lead to the formation of such free electrons.[5]

In principle, this approach can be used with all elements. In reality, however, current laser technology imposes some restriction on the range of elements that are actually amenable to this laser ionization based on resonance saturation (LIBORS) technique. The larger the energy gap being pumped the greater is the energy fed directly into the free electrons via superelastic collisions. Consequently, multiphoton saturation may be worth considering in certain instances.

We have shown elsewhere[6] that LIBORS appears to be particularly well suited for creating long plasma channels that will be needed for electron (or ion) beam transportation in certain future inertial fusion schemes. We have estimated that plasma channels of 5-m length with an electron density of about 10^{15} cm^{-3} could be created with less than 1 J of laser energy. We also believe that LIBORS could be used to create a charge exchange plasma that would be ideal for negative ion beam formation.

When this work was done all authors were with University of Toronto, Institute for Aerospace Studies, Downsview, Ontario M3H 5T6. N. Drewell is now at Atomic Energy of Canada, Chalk River, Ontario.

Received 16 August 1978.
0003-6935/79/111824-04$00.50/0.

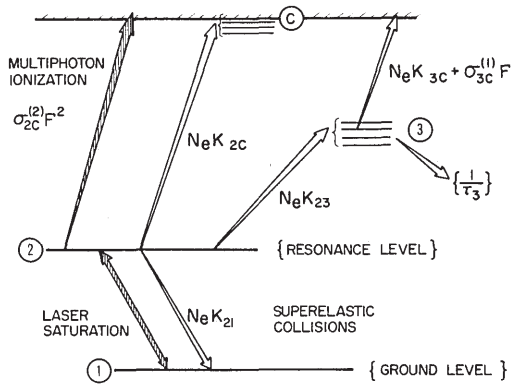

Fig. 1. Simple LIBORS model.

LIBORS Model and Calculations

Considerable physical insight into the various interactions arising when laser radiation is used to saturate a resonance transition can be gained by reference to Fig. 1. Under high density conditions (i.e., very short dephasing time), a rate equation analysis is applicable.[7] We have formulated a computer code that utilizes a 20-level model of the laser excited atom and have undertaken detailed calculations for the case of sodium vapor.[6,8]

Under saturating conditions, Measures[9] has shown that a population redistribution occurs between the two levels in a time

$$\tau_s \equiv [(1 + g_2/g_1)R_{21}]^{-1}, \tag{1}$$

where g_2 and g_1 represent the respective degeneracies of the upper and lower levels, and

R_{21} $\{\equiv B_{21} \int I^l(\nu)\mathcal{L}_{21}(\nu)d\nu/4\pi\}$ (sec^{-1}) represents the stimulated emission rate coefficient for the (2-1) resonance transition,

$I(\nu)$ represents the spectral irradiance of the radiation field at frequency ν appropriate to the resonance transition,

B_{21} represents the appropriate Milne coefficient, and

$\ell_{21}(\nu)$ represents the resonance line profile function.

The saturating condition can be expressed in the form: $I^l(\nu) \gg I_s(\nu)$, where the saturated spectral irradiance,

$$I_s(\nu) \equiv \frac{8\pi h\nu^3}{(1+g)c^2}\left\{\frac{\tau_2^{\text{RAD}}}{\tau_2}\right\}, \tag{2}$$

τ_2^{RAD} represents the radiative lifetime of the resonance transition $\{\tau_2^{\text{RAD}} = A_{21}^{-1}\}$,

$h\nu$ represents the laser photon energy $\{= E_{21}$, energy difference between levels 2 and 1$\}$,

c is the velocity of light,

$$\tau_2 \equiv \left[A_{21}^* + N_e\left\{K_{21} + K_{12} + \sum_{m>2} K_{2m}\right\}\right]^{-1} \tag{3}$$

represents the effective lifetime of the laser pumped level,[6]

A_{21}^* represents the effective resonance transition probability, allowing for self-absorption,[10]

N_e represents the free electron number density, and

$K_{\alpha\beta}$ represents the rate coefficient for electron collision induced transitions between levels α and β, respectively.

The ratio of the resonance to the ground state population densities closely approximates the infinite temperature limit, viz.,

$$\frac{N_2}{N_1} \approx \frac{g_2}{g_1} \equiv g \tag{4}$$

under conditions of saturation.

The energy equation for the free electrons can be divided into two equations, one for the growth of the free electron's mean translational energy ϵ_e, viz.,

$$\begin{aligned} N_e\frac{d\epsilon_e}{dt} &= N_eN_2K_{21}E_{21} + [2E_{21} - E_{c2} - \epsilon_e]N_2\sigma_{2c}^{(2)}F^2 \\ &+ \sum_{n\geq n^*}^{n=20}[E_{21} - E_{cn} - \epsilon_e]N_n\sigma_{nc}^{(1)}F + Q_{IB} \\ &+ N_e^3\sum_{n>1}^{n=20}K_{cn}(E_{cn} + \epsilon_e) \\ &- N_e\sum_{n\geq 1}^{n=20}N_nK_{nc}(E_{cn} + \epsilon_e) \\ &- N_eC - N_eN_aH_{ea} - N_e^2H_{ei}, \end{aligned} \tag{5}$$

where

$\sigma_{2c}^{(2)}$ $(\text{cm}^4\ \text{sec})$ represents the two-photon ionization rate coefficient for the resonance level,

F $(\text{photons cm}^{-2}\ \text{sec}^{-1})$ represents the laser photon flux density,

$\sigma_{nc}^{(1)}$ (cm^2) represents the cross section for single photon ionization. The sum extends over all $n \geq n^*$ for which single-photon ionization can be achieved;

Q_{IB} represents the volume heating rate arising from inverse bremsstrahlung[11];

K_{cn} represents the rate coefficient for a three-body recombination into level n;

N_eC represents the energy loss of the free electrons arising from the net upward movement of bound electrons due to inelastic collisions[8];

N_a represents the atom number density;

H_{ea} represents the free electron energy loss rate coefficient due to elastic collisions with atoms; and

H_{ei} represents the free electron energy loss rate coefficient arising from Coulomb scattering collisions with ions.[12]

The other equation governs the rate of growth of ionization, viz.,

$$\begin{aligned} \frac{dN_e}{dt} &= N_2\sigma_{2c}^{(2)}F^2 + \sum_{n\geq n^*}^{n=20}N_n\sigma_{nc}^{(1)}F + N_e\sum_{n\geq 1}^{n=20}N_nK_{nc} \\ &- N_e^2\sum_{n\geq 1}^{n=20}[N_eK_{cn} + \beta(n)], \end{aligned} \tag{6}$$

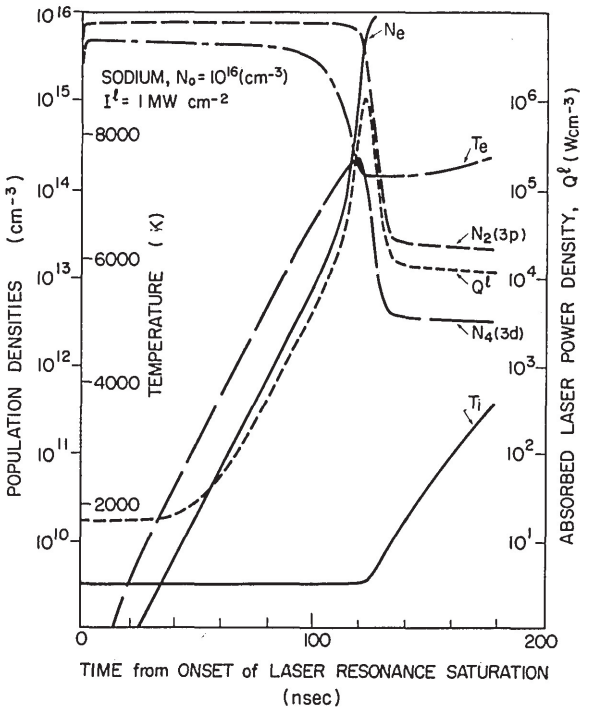

Fig. 2. Temporal variation of electron density N_e, electron temperature T_e, ion temperature T_i, $N_2(3p)$ resonance and $N_4(3d)$ excited state populations, and absorbed laser power density Q^l as predicted by LIBORS code for sodium with $N_o = 10^{16}$ (cm^{-3}) and $I^l = 10^6$ ($W\ cm^{-2}$).

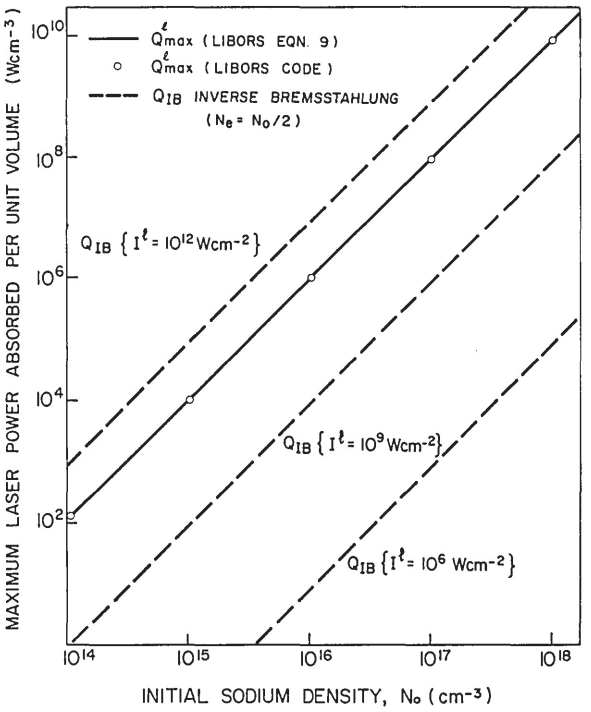

Fig. 3. Comparison of the variation in maximum laser energy deposition rate with initial sodium density as predicted by LIBORS code, simple LIBORS model, and for inverse bremsstrahlung (the latter for three values of laser irradiance).

where $\beta(n)$ represents the radiative recombination rate coefficient into level n.

The solution of Eqs. (5) and (6) in conjunction with the appropriate set of 20 population density equations[6,8] yields solutions such as those presented in Fig. 2. In this instance the initial sodium vapor density was assumed to be 10^{16} cm^{-3}, and the laser irradiance was taken to be 1 MW cm^{-2} at 589 nm consistent with the experiments of Lucatorto and McIlrath.[13] Two-photon ionization from the resonance level and single-photon ionization from $n > 3$ levels are taken into account.[8]

The particularly noteworthy features of this interaction are as follows: The electron temperature jumps, within a few nanoseconds of the redistribution of the population between the resonance and ground levels, to a plateau value that is in essence determined by a balance between collisional excitation and superelastic quenching of the resonance state.[4,8] Ionization proceeds with a rate that is first determined by two-photon ionization of the laser maintained resonance state population. (For lower laser power densities associative ionization might be significant.) Once the free electron density exceeds 10^{12} cm^{-3}, electron collisional ionization of the resonance level and single-photon ionization of the higher levels appear to take over and further accelerate the rate of ionization. During the final ionization burnout phase a momentary drop of the electron temperature is seen to be predicted.

Under saturating conditions, the attenuation of the laser beam can be expressed in the form[2,6]

$$dI^l(z)/dz = -Q^l \quad (W\ cm^{-3}), \tag{7}$$

where Q^l represents the net volume rate of power dissipation for the laser radiation and comprises the laser power dissipated in maintaining the resonance state population against (1) superelastic quenching [the first term on the right-hand side of Eq. (5) and represents the primary electron heating mechanism], (2) excitation to higher levels, and (3) spontaneous emission. The temporal variation of Q^l, at a sodium density of 10^{16} cm^{-3}, is shown in Fig. 2. Evidently, Q^l increases rapidly with increasing electron density reaching a peak just prior to ionization burnout. Our computer calculations clearly indicate that the superelastic heating term

$$Q^{SE} = N_e N_2 K_{21} E_{21} \tag{8}$$

dominates Q^l at this time (i.e., $N_2 \approx N_e \approx N_o/2$) in which case the relation

$$Q^l_{max} = G N_o^2 K_{21} E_{21}/4 \tag{9}$$

is closely approximated over several orders of magnitude variation in N_o, as seen by reference to Fig. 3 where $G \equiv (g_2/g_1)/(1 + g_2/g_1)$, and N_o represents the original sodium atom density prior to laser irradiation.

Q^l_{max} thus expresses the maximum rate of laser energy deposition into the plasma, and as such we wish to compare it with the rate of laser energy deposition via inverse bremsstrahlung,[11] viz.,

$$Q_{IB} = \frac{1.17 \times 10^{-7} N_o^2 \lambda^2 I^l}{12 c^2 (kT_e)^{3/2}}, \tag{10}$$

where we have assumed $N_e = N_o/2$ in order to make a comparison with $Q^l_{\max}$, λ(cm) represents the laser wavelength, T_e represents the electron temperature (with kT_e in eV), and I^l (W cm^{-2}) is the laser irradiance. A direct comparison of the rate of laser energy deposition through LIBORS and inverse bremsstrahlung can be obtained from the ratio of Eqs. (9) and (10), viz.,

$$H = \frac{Q^l_{\max}}{Q_{IB}} = \frac{(GN_o^2K_{21}E_{21}/4)12c^2(kT_e)^{3/2}}{1.17\times10^{-7}N_o^2\lambda^2I^l}. \quad (11)$$

The maximum value of laser irradiance needed in the LIBORS case to produce a deposition rate of $Q^l_{\max}$ over a plasma depth L is, from Eq. (7), simply $Q^l_{\max}L$. We can, for a given situation, deduce the minimum value of H (that is, the most conservative ratio) by setting

$$I^l = Q^l_{\max}L \quad (12)$$

in Eq. (11). Clearly, if we express

$$Q_{IB} = I^l/L_{IB}, \quad (13)$$

L_{IB} represents the characteristic absorption length for inverse bremsstrahlung. In which case we can write

$$H_{\min} = \frac{L_{IB}}{L} = \frac{12c^2(kT_e)^{3/2}}{1.17\times10^{-7}N_o^2\lambda^2L}. \quad (14)$$

$H_{\min}$ represents the minimum value for the rate of laser energy deposition via LIBORS along the path of the laser beam compared with inverse bremsstrahlung and is equal to the ratio given by Eq. (11) at the point of entry of the laser beam into the plasma. As the laser beam penetrates the plasma and is attenuated, the degree of coupling to the plasma via LIBORS is undiminished, but that through inverse bremsstrahlung decreases with I^l. Thus H increases with penetration through the plasma. Nevertheless, $H_{\min}$ is a useful quantity since it provides us with a conservative value for the advantage of LIBORS over inverse bremsstrahlung for a given situation, independent of the detail characteristics (such as G and K_{21}) of the particular atom being pumped. It should be noted that if excess laser power is available, such that $I^l \gg Q^l_{\max}L$, Eq. (11) has to be used, and $H_{\min}$ is no longer meaningful. Indeed as seen in Fig. 3, for very high values of I^l, $Q_{IB} > Q^l_{\max}$.

In the case of alkali metals, the laser wavelength will lie in the visible to near IR, and the appropriate value of kT_e will be around 1 eV. Indeed, for sodium, $\lambda = 589 \times 10^{-7}$ cm, and we may set $kT_e = 1$ eV. Under these circumstances,

$$H_{\min} \approx (2.66\times10^{37})/(N_o^2L), \quad (15)$$

and we can see that for typical plasmas ($L = 1$ cm), $H_{\min}$ can range from 2.66×10^9 at $N_o = 10^{14}$ cm^{-3} to 2.66×10^3 at $N_o = 10^{17}$ cm^{-3}.

Discussion and Conclusions

It is thus quite evident that LIBORS represents a mode of coupling laser energy into a plasma that can be many orders of magnitude greater than achieved through inverse bremsstrahlung for the same laser power. Put another way, LIBORS requires a much lower laser irradiance to accomplish the same rate of laser energy deposition into the plasma, or the effective absorption length for LIBORS is very much less than that for inverse bremsstrahlung. An additional attractive feature of the LIBORS approach is that it can be used in cases of a cold (i.e., un-ionized) gaseous medium.

It is also worth noting that if a laser is tuned to saturate a resonance transition of the singly charged ion, the superelastic heating term

$$Q^{SE} = N_eN_2^{II}K_{21}^{II}E_{21}^{II} \quad (16)$$

would be very large over the entire period to second stage ionization burnout, and not have just a sharp peak as indicated in the case of first stage ionization burnout. N_2^{II}, K_{21}^{II}, and E_{21}^{II} refer to the singly charged ion values of resonance state population density, superelastic collision rate coefficient, and resonance to ground energy separation.

Strontium represents an interesting candidate since resonance lines in both S_rI and S_rII (460.7 nm and 421.6 nm, respectively) could be pumped simultaneously by a dual wavelength flashlamp pumped dye laser. As shorter wavelength lasers become available, higher stages of ionization would become accessible to this LIBORS approach.

In summary the advantages of LIBORS over inverse bremsstrahlung as a means of coupling laser energy into a gaseous medium are:

(1) much higher rate of energy deposition;
(2) more efficient interaction;
(3) operates at much lower laser power levels;
(4) much shorter interaction length;
(5) laser beam attenuated linearly as energy deposition is uniform along the beam;
(6) cold start capability even at modest laser power levels.

It should also be noted that LIBORS can lead to almost complete ionization very much faster than the corresponding multiphoton rate. Of course all the above discussion relates to reasonably high density ($N_o > 10^{13}$) situations.

This work was supported by USAF/AFOSR under grant 76-2902B and the National Research Council of Canada.

References

1. K. W. Billman, Astronaut. Aeronaut., 56 (July 1975); L. K. Hansen and N. S. Rasor, "Thermo Electronic Laser Energy Conversion", 2nd NASA Laser Energy Conversion Conference, NASA-Ames, January 1975, NASA SP-395.
2. R. M. Measures, J. Quant. Spectrosc. Radiat. Transfer **10**, 107 (1970).
3. R. M. Measures, J. Appl. Phys. **48**, 2673 (1977).
4. R. M. Measures, N. Drewell, and P. Cardinal, "Superelastic Laser Energy Conversion (SELEC)", Prog. Astronaut. Aeronaut. **61**, 450 (1978).
5. A. V. Hellfeld, J. Caddick, and J. Weiner, Phys. Rev. Lett. **40**, 1369 (1978).
6. R. M. Measures, N. Drewell, and P. Cardinal, "Electron and Ion Beam Transportation Channel Formation by Laser Ionization Based on Resonance Saturation—LIBORS", J. Appl. Phys. (April 1979).
7. T. J. McIlrath and J. L. Carlsten, Phys. Rev A **6**, 1091 (1972).
8. R. M. Measures, N. Drewell, and P. Cardinal, "Rapid and Efficient Laser Ionization Based on Resonance Saturation" (in preparation).
9. R. M. Measures, J. Appl. Phys. **39**, 5232 (1968).
10. T. Holstein, Phys. Rev. **83**, 1159 (1951).
11. J. M. Dawson, Phys. Fluids **7**, 981 (1964).
12. E. J. Morgan and R. D. Morrison, Phys. Fluids **8**, 1608 (1965).
13. T. B. Lucatorto and T. J. McIlrath, Phys. Rev. Lett. **37**, 428 (1976); T. J. McIlrath and T. B. Lucatorto, Phys. Rev. Lett. **38**, 1390 (1977).